Light Scattering of Acetylated Lignin

GERHARD MERKLE,[1] SABINE AUERBACH,[1] WALTHER BURCHARD,[1,*]
ALBERT LINDNER,[2] and GERD WEGENER[2]

[1]Institute for Macromolecular Chemistry, University of Freiburg, W-7800 Freiburg, Germany, and
[2]Institute for Wood Research, University of Munich, W-8000 München 40, Germany

SYNOPSIS

Organosolv lignin was fractionated on a Sephadex G 75 column with 0.1 M aqueous NaOH resulting in 14 fractions. These fractions were acetylated and a high-molecular-weight fraction (F3) was investigated by means of combined static and dynamic light scattering (LS) in solvents acetone, tetrahydrofuran (THF), and trifluoroethanol (TFE). The measurements were found to be reproducible, and recycling of lignin by freeze drying caused slight but unessential changes in solution properties. Depending on the solvent used, weight average molecular weights M_w between two and ten million were found. By contrast, M_n of the fractions, measured by vapor pressure osmometry (VPO), was in the range of a few thousands only. Analysis of the angular dependence in static LS by means of a Casassa–Holtzer plot and the fractal dimensions showed the presence of chain stiffness, most distinct in TFE. Also, the dynamic light scattering results in TFE are typical for semiflexible chains, while in THF, and to some extent in acetone, the dynamic measurements including viscosity suggest the presence of spherical structures. These findings are being explained by large lignin clusters that consist of stiff subunits.

INTRODUCTION

Chemical pulping and bleaching is one of the essential procedures for the conversion of wood into paper. Mostly sulfurous components for pulping and chlorine containing chemicals in conventional bleaching sequences[1] create problems with respect to strict environmental regulations, especially in Germany.

Organocell, Gesellschaft für Zellstoff-und Umwelttechnik mbH, Munich, is among those companies that aim at a sulfurfree nonconventional pulping process, using methanol and sodium hydroxide as delignifying agents, which is to be implemented on an industrial scale until 1992.

The lignin obtained from this process is under discussion for high-value, nonenergetic uses. For this purpose, the chemistry and properties of this organosolv lignin had to be characterized.

For information on the chemical structure, Lindner und Wegener[2-5] studied Organocell lignins by means of elemental analysis, sugar analysis, IR, and nuclear magnetic resonance (NMR) spectroscopy, determination of functional groups, and controlled degradation experiments. Vapor pressure osmometry, gel permeation chromatography (GPC) and high-pressure scanning electron chromatography (SEC) (HPSEC) were performed to determine molecular weight and molecular weight distributions. For different soluble and residual lignins, they found molecular weight distributions covering the range between 300 and 30,000, using polystyrene standards for a calibration curve.[4] Since hydrodynamic properties of polystyrene and lignin are obviously quite different, a method for absolute molecular weight determination is required.

One of these absolute techniques is given by common or static light scattering (LS). Since only low molecular weights were expected, static LS would give no information on the structure. Hydrodynamically equivalent sphere radii can, however, be obtained by using dynamic LS, which permits the determination of diffusion coefficients. From this, the mentioned hydrodynamic radius is obtained via the Stokes–Einstein relationship. The experiments

* To whom correspondence may be addressed.

Journal of Applied Polymer Science, Vol. 45, 407–415 (1992)
 CCC 0021-8995/92/030407-09$04.00

gave rather unexpected but reproducible results.[a] We consider it informative to report on these data, although at the present stage we cannot yet offer a comprehensive explanation of the observed phenomena.

EXPERIMENTAL

Materials

Spruce wood lignin was obtained from a demonstration plant (5 tons of pulp per day, Organocell GmbH, Munich). A detailed description of the process, isolation, fractionation, and acetylation of lignin is given elsewhere,[2-5] while a brief description is given below.

Isolation of Lignin

The Organocell process works in two steps. Spruce chips are cooked at 185°C in a methanol–water mixture (50/50 s/s). After evaporating methanol from the liquor, lignin remains insoluble in the water phase and can be isolated by centrifugation (first-stage lignin).

In the second stage, pulping is performed at 170°C for about 40 min in a methanol–water mixture (30/70 s/s) with addition of NaOH (about 10% related to dry wood). This extract contains most of the lignin, which, after evaporation of methanol, is obtained by precipitation with acid or by electrolysis (second-stage lignin). The sample used for these experiments was a second-stage lignin recovered by acid precipitation (Sp S/DA1).

Fractionation

Fractionation of this lignin was carried out by means of GPC. A 2.4 × 130 cm column was filled with Sephadex G 75 and 0.5 g lignin were eluated in 14 fractions (F1–F14) with 0.1 *M* aqueous NaOH. After precipitation with 1.5 *M* HCl (at pH = 2), centrifugation, washing with water, and freeze drying, the lignin fractions were acetylated. The fraction F3 was used for LS experiments. M_w of this fraction was 11,900 and M_n (by HPSEC) 6,200 yielding a dispersity factor of 1.92.

The column was calibrated with polystyrene standards (molar mass *M* between 2400 and 35,000), curcumin (M = 370), and vanillin (M = 152).

[a] This means ±10% in M_w, ±8% in $\langle S^2 \rangle_z$, and ±3% in D_z.

Acetylation

200 mg lignin were dissolved in 1 mL pyridine. After addition of 1 mL acetic anhydride, the solution was kept under nitrogen for 24 h at 45°C. 1 mL methanol and 8 mL CH_2Cl_2 were added and the product was then extracted with 2 *M* HCl. The organic phase was dried over Na_2SO_4 and lignin was isolated by evaporation of the solvent.

Light Scattering

Solutions were prepared by dilution from stock solutions with p.a. grade solvents acetone, tetrahydrofuran (THF), and trifluoroethanol (TFE) and filtered in a laminar flow cabinet through 1.2 μm PTEF filter (Sartorius) into dust-free cylindrical quartz cells.

Static and dynamic LS measurements were carried out simultaneously using a krypton-ion-laser (647.1 nm, Spectra Physics No. 2020) in the angular range of 20–150° in steps of 10°. An ALV-3000 goniometer system (ALV-Langen) with an automatic drive equipped with an ALV-structurator-correlator was used. Details of the instrument and of the data evaluation are given in ref. 6.

The measurements were performed at 20°C with five concentrations in the range from 1 to 10 g/L in solvents acetone, THF, and TFE. To test reproducibility of measurements, some THF solutions were evaporated, lignin was freeze dried from 1.4-dioxane, and measurements were again performed in THF. By contrast, recycled polymer from TFE solutions was no longer soluble in THF.

Refractive index increments were measured with a Brice–Phoenix differential refractometer in solvents acetone and THF. Refractive index increment in TFE was obtained by plotting the obtained dn/dc values in acetone and THF vs. the refractive index of the solvents and extrapolating to the refractive index of TFE. The obtained values, together with the refractive indices of the solvents, are listed in Table I.

UV-Vis-Spectroscopy Measurements

All solutions were brown and showed a slight absorption at 647 nm, the wavelength of incident light. The optical density of each solution was measured at 647 nm in 1-cm quartz cells with a UV-Vis-spectrophotometer (Perkin-Elmer 330), and this absorption was taken into account in the LS measurements by dividing the scattered intensities by this angle-independent factor.

Table I Refractive Index Increments (dn/dc) of Lignin in Different Solvents (λ = 647 nm, T = 20°C), Refractive Indices (n), and Viscosities of Solvents (η)

	Solvent		
	Acetone	THF	TFE
dn/dc (mL/g)	0.139	0.180	0.238
n	1.407	1.358	1.291
η (cp)	0.324	0.486	1.75

After filtration of solutions for LS, some residual traces were observed in the filter. Concentrations were checked by measuring optical density at 647 nm before and after filtration. With the aid of a calibration curve obtained from nonfiltered lignin solutions, it was possible to determine the actual concentrations. A loss of about 10% was found. This check was not done for measurements in acetone and THF, but a comparison of corrected and uncorrected results showed that there was no essential change due to this systematic concentration error.

Viscosity Measurements

The intrinsic viscosity [η] was measured in solvents acetone and THF with an automatic Ubbelohde viscosimeter (Schott) in the concentration range of 1–10 g/L.

RESULTS

First evaluations of LS data in Zimm plots provide six quantities that give information about the dilute solution behaviour of the polymer. These are in static light scattering (SLS) the weight average molecular weight M_w, the z-average of mean square radius of gyration $\langle S^2 \rangle_z$ from the angular dependence, and the second virial coefficient A_2 from the concentration dependence at zero angle.

Analogous treatment of the dynamic data (DLS), i.e., $D_{app} = \Gamma/q^2$ in a dynamic Zimm plot[7,8] leads to the z-average diffusion coefficient,[9] the C-parameter, which is structure related, and k_d, which is useful for analysis of frictional properties. Here, $q = (4\pi/\lambda) \sin(\theta/2)$ is the magnitude of the scattering vector, which is related to the wavelength of the light in the solvent and the scattering angle θ. Γ is the initial slope of the logarithmic time correlation function $g_1(t)$,[10] i.e., $\Gamma = -(\mathrm{d} \ln g_1(t)/\mathrm{d}t)$, at $t = 0$.

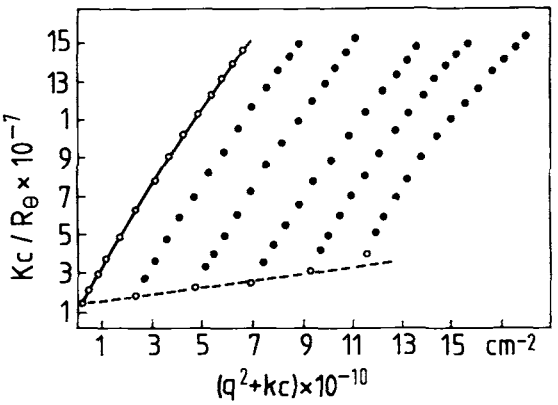

Figure 1(a) Static Zimm plot of the LS measurements from acetylated lignin in acetone; c = 1, 2, 3, 4, 5 g/L. K^* denotes the optical contrast factor K multiplied by $(T/100)^{0.8}$ for correction of the absorption at 647.1 nm. T is the measured transmission for each concentration; the factor 0.8 results from geometry of LS and UV spectroscopy cells.

Figures 1(a) and (b) show a static and a dynamic Zimm plot, respectively, from sample F3 in acetone.

SLS

Table II lists the results obtained from static Zimm plots for the three solvents and for the recycled sample, which is marked by the suffix r. R_g is the square root of the z-average mean square radius of gyration $R_g = (\langle S^2 \rangle_z)^{1/2}$.

For further examination of the particle-scattering factor $P(q)$, the LS data, obtained from extrapolation to concentration $c = 0$, were plotted as $P(q)^*q$ vs. $u = R_g{}^*q$.

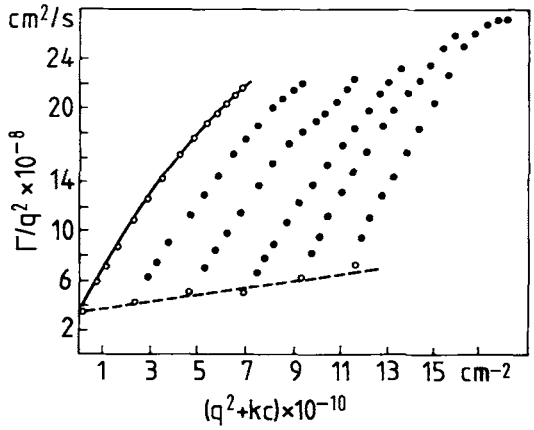

Figure 1(b) Dynamic Zimm plot of the LS measurements from acetylated lignin in acetone.

Table II Molecular Weight M_w, Radius of Gyration R_g, and Second Virial Coefficient A_2 from Static Zimm Plots in the Three Solvents and Chain Parameters Obtained from BR Plots

	Solvent			
	Acetone	TFE	THF	THF*r*
$M_w * 10^{-6}$ (mol/g)	9.7	1.9	3.6	5.26
A_2 (mol mL/g^2) $* 10^4$	2.5	2.38	2.32	0
R_g (exp)(nm)	285	140	154	135
R_g (cal)(nm)	305	150	152	136
l_k (nm)	188	200	163	45
N_k (nm)	9.2	2.25	4.3	38
L_w (nm)	1730	450	700	1700
z	0.1	0.01	0.95	1
M_L [g/(mol*nm)]	5600	3900	5400	3100

R_g (cal) is the radius of gyration calculated from parameters.[14] The suffix *r* denotes "recycled."

The particle-scattering factor is defined by:

$$P(q) = i(\theta)/i(0), \qquad (1)$$

where $i(\theta)$ is scattered intensity at observed angle θ and $i(0)$ the intensity at angle zero. In this so-called bending rod or Casassa–Holtzer plot (BR plot),[11,12] the curves for flexible chains pass through a maximum at small q-values and show a $1/q$ dependence at larger q-values. Rodlike molecules reach a plateau value without passing through a maximum, while semiflexible chains pass through a maximum before they turn into a plateau. Figure 2 schematically shows scattering behavior of flexible, semiflexible, and rodlike molecules.

The rod plateau is a measure of the mass per unit length M_L and is independent of a chain length polydispersity, while the position of the maximum depends on chain length polydispersity. The ratio of the maximum height to asymptote is a function of both chain stiffness and polydispersity. With the aid of relationships, which were published by Schmidt et al.[13] and further developed by Denkinger and Burchard,[14,15] the contour length $L_w = M_w/M_L$, the Kuhn segment length l_K,[14,15] and the polydispersity parameter z of the polymer can be determined. Since $1/z = (M_w/M_n) - 1$, large values of z represent monodisperse systems and $z = 1$ describes a Schulz–Flory most probable distribution with $M_w/M_n = 2$. Table II gives the parameters obtained from BR plots. Figure 3 shows the BR plots of lignin in different solvents; the full lines were calculated from the Koyama approximation[16] with the parameters as listed in Table II. As outlined in the discussion, these findings indicate rigid needle-like *internal* structures, but they give no information how these are clustered together. This is obtained from viscosity and dynamic light scattering.

Fractal Dimensions

For structures where the density is dependent on the mass of a particle, the scattered intensity is a function of the scattering angle and often follows a power law of the kind[17]

$$I(q) \sim q^{-D}. \qquad (2)$$

Here, D is the fractal dimension, which relates mass M to radius R

$$M \sim R^D. \qquad (3)$$

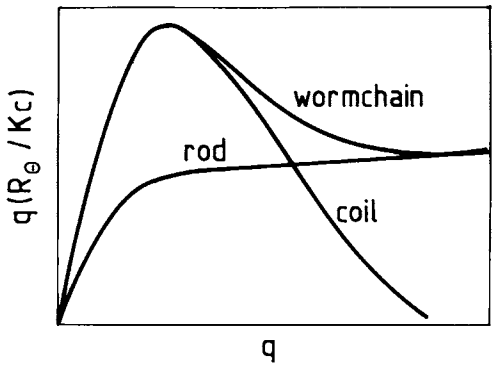

Figure 2 Coil, rod, and wormlike chain in an idealized Casassa–Holtzer plot (BR plot).

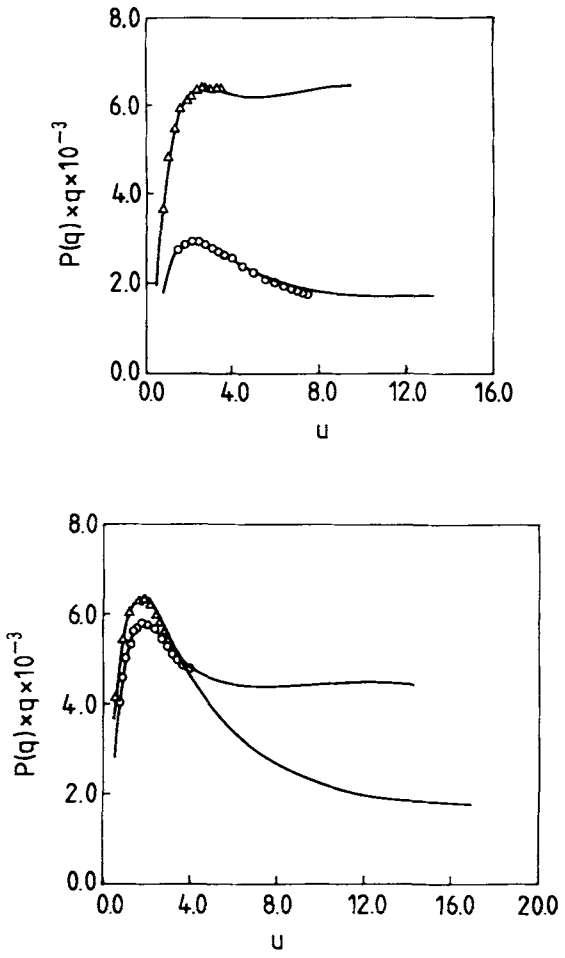

Figure 3 BR plot from LS data of acetylated lignin in (**a**) ○ acetone, △ TFE, (**b**) ○ THF and △ the recycled sample in THF. Full lines were calculated according to the Koyama approximation with the set of parameters as given in Table II. The undulation of the calculated curve in the case of TFE solution is an artefact of the Koyama theory, which combines two particle-scattering functions (flexible chain and stiff rod) to a hybrid function.

Systems that can be described by such a power law are called mass fractals and show slopes between −1 and −3, depending on the structure of the system, but D may be noninteger. Table III shows some theoretically derived exponents and the fractal dimensions for the fraction F3 that were obtained from the slope in a double-log plot of scattered intensity vs. q. (See Figure 4.)

It should be mentioned that such interpretation of static LS data is applicable only in a region, where $1/q$ is smaller than ξ, the correlation range of the system.[19] The fractal dimension D for branched or crosslinked chains is also affected by a size polydispersity of the system and in general reduces its value.

Dynamic LS

Intensity fluctuations of the scattered light, measured with a photomultiplier tube and analyzed with a fast computer, give a possibility to determine the relaxation time spectrum of a system under equilibrium conditions or the diffusion coefficient D_z, depending on the way data are evaluated. The diffusion coefficients measured at concentration c and angle θ can be extrapolated to zero concentration, which yields the translation diffusion coefficient D_z^0. Apparent diffusion coefficients can also be determined at a finite scattering angle. For particles not larger in diameter than the wavelength of the applied light, the concentration and angular dependencies can be described by the following equations[8]:

concentration dependence at zero angle

$$D_c = D_z^0(1 + k_D c + \cdots) \tag{4}$$

angular dependence at zero concentration

$$D_{app}(q) = D_z^0(1 + Cq^2\langle S^2\rangle - \cdots). \tag{5}$$

The parameter k_D is connected to A_2 and the frictional coefficient k_f by irreversible thermodynamics as follows[20-23]:

$$k_f = 2A_2M_w - k_D - v_2 \tag{6}$$

$$f_c = f_0(1 + k_f c) \tag{7}$$

$$k_f = k_{f0}V_h(N_A/M_w), \tag{8}$$

with v_2 the partial specific volume and V_h the hydrodynamic volume (defined by R_h) of the polymer in solution. From this and eq. (4), it is seen that the translation diffusion coefficient at finite concentrations is governed by the largely counterbalancing hydrodynamic and thermodynamic effects. The di-

Table III Fractal Dimensions D Measured in Different Solvents and Theoretical Calculated Values for Various Structures[18]

Sample	D
F3 in acetone	+1.44
F3 in THF	+1.32
F3 in TFE	+1.0
Linear ideal polymer (random walk)	+2
Linear swollen polymer (self-avoiding walk)	+5/3
Swollen branched polymer	+2
Randomly branched ideal polymer	+16/7

mensionless parameter C is characteristic of the molecular architecture and essentially represents the influence of the slowest mode of internal motions.[24] According to Stokes and Einstein, an equivalent hard sphere hydrodynamic radius R_h can be defined:

$$D = kT/6\pi\eta R_h, \quad (9)$$

with k the Boltzmann constant, T the absolute temperature, and η the viscosity of solvent.

The ratio of the geometrically defined radius of gyration R_g and the hydrodynamic radius is the ρ-parameter, which is sensitive to polymer architecture, but its value depends not only on structure but also on polydispersity, chain stiffness, and excluded volume. The experimentally found ρ-parameters observed with the present lignin acetate system are listed in Table IV with other characteristic data measured by dynamic LS.

Viscosity Measurements

Intrinsic viscosities were obtained from the plot of reduced viscosities η_{sp}/c vs. c and extrapolation to zero concentration. Mostly, a straight line is obtained that follows the relationship:

$$\eta_{sp}/c = [\eta] + k_h[\eta]^2 c, \quad (10)$$

in which k_h is the Huggins constant.

Intrinsic viscosities and Huggins coefficients were 5.5 mL/g, 0.61 and 6.8 mL/g, 0.9 in THF and acetone, respectively.

DISCUSSION

Three most striking features were found:

1. The weight average molecular weights M_w are unexpectedly high and in no way comparable with the number average molecular weights (M_n) measured by VPO and HPSEC.
2. The scattering behaviour depends on the solvent used.
3. Intrinsic viscosities in THF and acetone are rather low, considering the high molecular weight.

These findings are clear evidences of aggregation.

Research on lignin has shown that association and aggregation[26] seem to be characteristic properties of lignin solutions, no matter whether the lignins are kraft lignins,[26–31] organosolv lignins,[32] or acetylated lignins.[33] Therefore, it is not surprising to find different molecular weights in different solvents.

Table IV Parameters Obtained from DLS

	Solvent			
	Acetone	TFE	THF	THFr
D_z° (cm²/s)*10⁸	3.8	1.4	2.8	2.85
R_h (nm)	177	87	158	155
ρ	1.61	1.61	0.98	0.87
k_d (mL/g)	83	20	143	100
k_{f0}	0.28	0.08	0.001	−0.06
C	0.09	0.2	0.34	0.24

Most studies concerning molecular weights and molecular weight distributions were carried out with kraft lignins in buffered aqueous solutions. LS measurements of fractionated alkali lignins in $NaHCO_3$–NaOH buffer (pH = 9.65) were performed as early as 1960, yielding a molecular weight range from 50,000 to $48*10^6$ and a hydrodynamic behaviour between that of a solid sphere and a Gaussian coil.[34] These results are all the more remarkable as alkali lignins are gained under delignification conditions that bear a certain resemblance to the second stage of the Organocell process. M_w values of up to 138,000 were determined for lignosulfonate fractions by means of LS in aqueous solution.[35]

To improve GPC column calibration of Sephadex G75/NaOH systems, Forss et al.[36] used narrow lignosulfonate fractions for column calibration, the molecular weight of which was determined by either LS or sedimentation velocity. The results obtained by those different techniques correspond reasonably well. M_w values obtained by LS ranged from about 10,000 to 75,000.

Recently, interest in LS was revived by Froment and Pla,[37] who found M_w values ranging from 4,700 to 55,000 for alkali lignin fractions from Black Cottonwood. These authors also report about on-line size-exclusion-chromatography/low-angle laser light-scattering equipment that allows the continuous calculation of M_w from molecules eluting from a set of columns, thereby avoiding the well-known problems of column calibration.

Dutta et al.[38] made LS measurements of kraft lignin association complexes in DMF at 514.5 nm obtaining M_w values up to $8.7*10^6$.

At present, we are not able to explain the startling differences between the various experimental data.

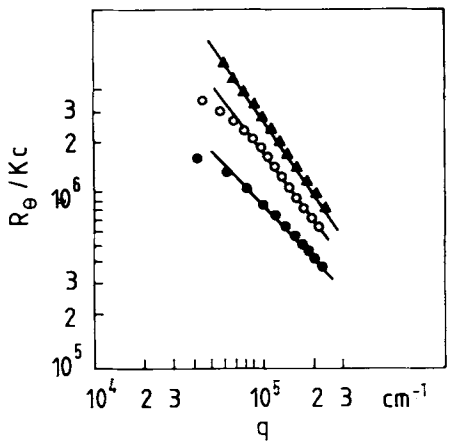

Figure 4 Double-log plot from scattering intensities as R_θ/Kc vs. scattering vector q for acetylated lignin in (●) TFE, (○) THF, and (▲) acetone. The slope gives D, the fractal dimension of the substructures in the particle.

We will now confine the discussion to the structures observed by LS. Analysis of the form factor $P(q)$ gives information on chain stiffness and polydispersity.[13–15] In all solvents used, lignin exhibits a scattering behaviour characteristic of semiflexible chains. The curves were fitted by Koyama approximation[16] and the strongest chain stiffness was found in TFE with a Kuhn segment length l_k = 200 nm and n_k = 2.3 Kuhn segments. In acetone and THF, the molecules are more flexible (Table II).

Similar conclusions are obtained from the measured fractal dimensions. The slope of −1, i.e., $D \approx 1$ in a double-logarithmic plot of scattering intensity in TFE against q is a strong indication of the presence of stiff linear objects. The enlarged slopes in THF and acetone are in accordance with the more flexible character of the particles in these solvents. (Figure 4.)

Frictional properties are reflected by the value of k_{f0}. The constant k_{f0} is high for noninterpenetrating spheres (k_{f0} = 7.8–8.0) and small for flexible chains in the θ-state, where almost complete interpenetration occurs (k_{f0} = 2.23).[20–23] The experimental values obtained from lignin solutions are very small and outside the usual range (Table IV). Similar data were also observed in LS measurements from Tamarind gum (a native polysaccharide from tamarind seed) by Lang.[39] Tamarind gum likewise has tendency to form associates and exhibits chain stiffness.

More information is available by combining DLS and SLS results, which leads to the ρ-parameter and, from the angular dependence of DLS, to the C-parameter (Table V). Comparison of these parameters with theoretical values calculated for different structures leads to the conclusion that rather flexible and, for the THF solutions, even spherical structures exist.

Also, the viscosity measurements suggest the presence of spherical particles since the obtained low intrinsic viscosities and the virtual independence of concentration are characteristic of spherical structures.

These findings do not necessarily contradict one another. We have to keep in mind that the intrinsic viscosity is a global structural parameter sensitive to the volume of the particle per mass of the particle,[40] i.e., $[\eta] \sim V_h/M$. This quantity tells us something about the overall segment density but nothing about how these segments are arranged within the volume and whether these segments are flexible or rigid and needle-like.

All scattering techniques provide us with the capability to look inside a particle, as long as the particles diameter is much larger than the wavelength[41] (more accurate if $Rg*q \gg 1$). Static LS shows a semiflexible, chainlike *internal* structure. These substructures could be rigidly frozen bent rods, or these structures may have some mobility left. The data for the C-parameter gives information on an inherent internal mobility.[24] A nearly zero value for C indicates a rigid frozen-in structure, but the observed data are, with the exception of the acetone solution, close to the values for flexible linear or randomly branched chains. (Compare Table IV and Table V.) Hence, the aggregation is not rigid as in inorganic colloids but apparently has the high flexibility of typical macromolecules.[8]

Putting all facts together, we arrive at the following picture. The lignin fractions (of low molecular weight) have a strong tendency to cluster together

Table V ρ-Parameters and C-Parameters for Some Selected Structures[8,25]

Architecture	ρ	C
Homogeneous sphere	0.778	0
Random coil, monodisperse		
0-conditions	1.5	0.173
Good solvent	1.78	—
Random coil, polydisperse z = 1		
0-conditions	1.73	0.200
Good solvent	2.05	—
Rigid rod, infinitely thin		
Monodisperse, $z = \infty$	>2.00	0.042
Polydisperse, z = 1	>2.00	0.16

and form huge aggregates. This does not occur in random fashion, but there is a high preference for forming longish worm-like sections. These worm-like linear substructures are not frozen in but guarantee a rather high flexibility of the overall particle structure. This overall or global structure resembles the randomly aggregated structure in acetone and TFE, whereas in THF a sphere-like structure is obtained.

TFE is certainly the best H-bond breaking reagent applied in this study. Therefore, it can break junctions consisting of only a few H-bonds in a row, which cannot be cracked by acetone or THF. The result will be a thinning of the highly disordered bundles, resulting in a lower fractal dimension close to unity. It was exactly this behaviour that was observed experimentally (see Table III). A recycling of acetylated lignin from these solutions apparently induces the fibrillar substructures to aggregate laterally, and now too many H-bonds are formed in a row such that THF is no longer able to break up the junctions: The material remains insoluble.

The nature of intermolecular forces is still under discussion.[27] Since we have investigated an acetylated sample, hydrogen bonding from phenolic hydroxyl groups should be discounted. On the other hand, in a solvent well known to prevent hydrogen bonding, the lowest molecular weight is observed. Therefore, in this case, the reason for association is still questionable.

Sarkanen et al.[32] explain the presence of kraft lignin association complexes in alkaline solutions by means of HOMO–LUMO interactions (interactions of the highest occupied molecular orbital with the lowest unoccupied molecular orbital). In contrast to hydrogen bonding, HOMO–LUMO interactions would also affect fully acetylated lignins.

One other problem remains unsolved. According to GPC, the lignin acetate should have a low molecular weight. Although the GPC analysis with a column that has been calibrated by linear polystyrene will lead to large errors by a factor of about 100, it remains unexpected to find masses of more than $5*10^6$. Apparently, the fractionation mechanism from highly branched or aggregated structures is not yet fully understood. Similar effects were also recently observed with pectins.[42] The low number average molecular weight is not in variance with the high molecular weight average M_w because all branching and aggregation theories predict huge polydispersity that, eventually, at a critical point diverges.[43–45]

REFERENCES

1. D. Fengel and G. Wegener, *Wood—Chemistry, Ultrastructure, Reactions,* W. de Gruyter, Berlin, 1984, 1989.
2. A. Lindner and G. Wegener, *J. Wood Chem. Tech.*, **8,** 323 (1988).
3. A. Lindner and G. Wegener, *J. Wood Chem. Tech.*, **9,** 421 (1989).
4. A. Lindner and G. Wegener, *J. Wood Chem. Tech.*, **10,** 331 (1990).
5. A. Lindner and G. Wegener, *J. Wood Chem. Tech.*, **10,** 351 (1990).
6. S. Bantle, M. Schmidt, and W. Burchard, *Macromolecules,* **15,** 1604 (1982).
7. W. Burchard, M. Schmidt, and W. H. Stockmayer, *Macromolecules,* **13,** 580 (1980).
8. W. Burchard, M. Schmidt, and W. H. Stockmayer, *Macromolecules,* **13,** 1265 (1980).
9. A. Z. Akcasu, M. Benmouna, and C. C. Han, *Polymer,* **21,** 866 (1980).
10. J. B. Berne and R. Pecora, *Dynamic Light Scattering,* Wiley, New York, 1974.
11. A. J. Holtzer, *J. Polym. Sci.,* **17,** 432 (1955).
12. E. F. Casassa, *J. Chem. Phys.,* **23,** 596 (1955).
13. M. Schmidt, G. Paradossi, and W. Burchard, *Macromol. Chem. Rapid Commun.,* **6,** 767 (1985).
14. P. Denkinger and W. Burchard, *J. Polym. Sci., Polym. Phys. Ed.,* **29,** 589 (1991).
15. W. Burchard and P. Denkinger, in *Proceedings of 2nd Dresdener Polymer Discussion,* Gaussich, 1989.
16. R. Koyama, *J. Phys. Soc. Jpn.,* **34,** 1029 (1973).
17. D. W. Schaefer, J. E. Martin, A. J. Hurd, and K. D. Keefer, in *Physics of Finely Divided Matter,* N. Boccara and M. Daoud, eds., Springer, Berlin, 1985.
18. M. Daoud and F. Family, *J. Phys. (Paris),* **42,** 1359 (1981).
19. D. W. Schaefer and K. D. Keefer, *Mater. Res. Soc. Symp. Proc.,* **32,** 1 (1984).
20. H. Yamakawa, *J. Chem. Phys.,* **36,** 2995 (1962).
21. C. W. Pyun and M. Fixman, *J. Chem. Phys.,* **41,** 937 (1964).
22. S. Imai, *J. Chem. Phys.,* **41,** 937 (1964).
23. A. Z. Akcasu and M. Benmouna, *Macromolecules,* **11,** 1193 (1978).
24. M. Schmidt and W. H. Stockmayer, *Macromolecules,* **17,** 509 (1984).
25. W. Burchard, *Adv. Polym. Sci.,* **48,** 1 (1983).
26. T. Lindström, *Colloid Polym. Sci.,* **257,** 277 (1979).
27. D. L. Woerner and J. L. McCarthy, *Macromolecules,* **21,** 2160 (1988).
28. S. Sarkanen, E. Abramowski, and J. L. McCarthy, *Macromolecules,* **15,** 1098 (1982).
29. W. J. Connors, S. Sarkanen, and J. L. McCarthy, *Holzforschung,* **34,** 80 (1980).
30. W. Brown, *J. Appl. Polym. Sci.,* **11,** 2381 (1967).
31. K. G. Forss, B. G. Stenlund, and P. E. Sågfors, *Appl. Polym. Symp.,* **28,** 1185 (1976).

32. S. Sarkanen, D. T. Teller, J. Hall, and J. L. McCarthy, *Macromolecules,* **14,** 426 (1981).
33. S. Sarkanen, D. C. Teller, C. R. Stevens, and J. L. McCarthy, *Macromolecules,* **17,** 2588 (1984).
34. P. R. Gupta and D. A. I. Goring, *Can. J. Chem.,* **38,** 270 (1960).
35. J. Moacanin, V. F. Felicetta, W. Haller, and J. L. McCarthy, *J. Am. Chem. Soc.,* **77,** 3470 (1955).
36. K. Forss, R. Kokkonen, and P.-E. Sågfors, in *Lignin: Properties and Materials,* W. G. Glasser and S. Sarkanen, eds., ACS Symposium Series 397, American Chemical Society, Washington, DC, 1988, pp. 124–133.
37. P. Froment and F. Pla, in *Lignin: Properties and Materials,* W. G. Glasser and S. Sarkanen, eds., ACS Symposium Series 397, American Chemical Society, Washington, DC, 1988, pp. 135–143.
38. S. Dutta, T. M. Garver, and S. Sarkanen, in *Lignin: Properties and Materials,* W. G. Glasser and S. Sarkanen, eds., ACS Symposium Series 397, American Chemical Society, Washington, DC, 1988, pp. 155–176.
39. P. Lang, PhD Thesis, University of Freiburg, 1991.
40. T. G. Fox Jr. and P. J. Flory, *J. Am. Chem. Soc.,* **73,** 1904 (1951).
41. M. B. Huglin, *Light Scattering from Polymer Solutions,* Academic Press, New York, 1972.
42. B. Haesslin and W. Burchard, unpublished data.
43. W. H. Stockmayer, *J. Chem. Phys.,* **11,** 45 (1943).
44. W. H. Stockmayer, *J. Chem. Phys.,* **12,** 125 (1944).
45. D. Stauffer, *Introduction to Percolation Theory,* Taylor and Francis, London, 1985.

Received February 26, 1991
Accepted July 19, 1991